



Serpentoviruses: More than Respiratory Pathogens

Eva Dervas,^a  Jussi Hepojoki,^{a,b} Teemu Smura,^b Barbara Prähauser,^a Katharina Windbichler,^a Sandra Blümich,^a Antonio Ramis,^c Udo Hetzel,^a  Anja Kipar^a

^aInstitute of Veterinary Pathology, Vetsuisse Faculty, University of Zürich, Zürich, Switzerland

^bUniversity of Helsinki, Medicum, Department of Virology, Helsinki, Finland

^cServei de Diagnostic en Patologia Veterinaria (SDPV), Departament de Sanitat i Anatomia Animals, Facultat de Veterinària, Universitat Autònoma de Barcelona, Barcelona, Spain

ABSTRACT In recent years, nidoviruses have emerged as important respiratory pathogens of reptiles, affecting captive python populations. In pythons, nidovirus (recently reclassified as serpentovirus) infection induces an inflammation of the upper respiratory and alimentary tract which can develop into a severe, often fatal proliferative pneumonia. We observed pyogranulomatous and fibrinonecrotic lesions in organ systems other than the respiratory tract during full postmortem examinations on 30 serpentovirus reverse transcription-PCR (RT-PCR)-positive pythons of varying species originating from Switzerland and Spain. The observations prompted us to study whether this not yet reported wider distribution of lesions is associated with previously unknown serpentoviruses or changes in the serpentovirus genome. RT-PCR and inoculation of *Morelia viridis* cell cultures served to recruit the cases and obtain virus isolates. Immunohistochemistry and immunofluorescence staining against serpentovirus nucleoprotein demonstrated that the virus infects not only a broad spectrum of epithelia (respiratory and alimentary epithelium, hepatocytes, renal tubules, pancreatic ducts, etc.), but also intravascular monocytes, intralésional macrophages, and endothelial cells. With next-generation sequencing we obtained a full-length genome for a novel serpentovirus species circulating in Switzerland. Analysis of viral genomes recovered from pythons showing serpentovirus infection-associated respiratory or systemic disease did not reveal sequence association to phenotypes; however, functional studies with different strains are needed to confirm this observation. The results indicate that serpentoviruses have a broad cell and tissue tropism, further suggesting that the course of infection could vary and involve lesions in a broad spectrum of tissues and organ systems as a consequence of monocyte-mediated viral systemic spread.

IMPORTANCE During the last years, python nidoviruses (now reclassified as serpentoviruses) have become a primary cause of fatal disease in pythons. Serpentoviruses represent a threat to captive snake collections, as they spread rapidly and can be associated with high morbidity and mortality. Our study indicates that, different from previous evidence, the viruses do not only affect the respiratory tract, but can spread in the entire body with blood monocytes, have a broad spectrum of target cells, and can induce a variety of lesions. *Nidovirales* is an order of animal and human viruses that comprises important zoonotic pathogens such as Middle East respiratory syndrome coronavirus (MERS-CoV), severe acute respiratory syndrome coronavirus (SARS-CoV), and SARS-CoV-2. Serpentoviruses belong to the same order as the above-mentioned human viruses and show similar characteristics (rapid spread, respiratory and gastrointestinal tropism, etc.). The present study confirms the relevance of natural animal diseases to better understand the complexity of viruses of the order *Nidovirales*.

Citation Dervas E, Hepojoki J, Smura T, Prähauser B, Windbichler K, Blümich S, Ramis A, Hetzel U, Kipar A. 2020. Serpentoviruses: more than respiratory pathogens. *J Virol* 94:e00649-20. <https://doi.org/10.1128/JVI.00649-20>.

Editor Julie K. Pfeiffer, University of Texas Southwestern Medical Center

Copyright © 2020 American Society for Microbiology. All Rights Reserved.

Address correspondence to Anja Kipar, anja.kipar@uzh.ch.

Received 9 April 2020

Accepted 2 July 2020

Accepted manuscript posted online 8 July 2020

Published 31 August 2020

KEYWORDS granulomatous inflammation, serpentoviruses, systemic viral infection, vasculitis, viremia

In the past, toroviruses, a subfamily of the order *Nidovirales*, were mainly known to cause enteric disease in mammals (1–4). Recent studies linked nidovirus infections to respiratory disease in cattle, pythons, and lizards, thus establishing nidoviruses as respiratory pathogens (5–12). In pythons, nidoviruses were found to be associated with chronic proliferative pneumonia (5, 6, 10, 11), and the association was confirmed by experimental infection studies (7). Severe cases exhibit typical pathological changes after both experimental and natural infection; these include stomatitis, rhinitis, tracheitis, and pneumonia with significant mucus accumulation. Taxonomically, python nidoviruses have recently been reclassified into the family *Tobaniviridae*, subfamily *Serpentovirinae*, genus *Pregotovirus* (International Committee on Taxonomy of Viruses [ICTV]; <https://talk.ictvonline.org> [July 2018]).

A recent study identified yet another new nidovirus (genus *Barnivirus*) in Bellinger River snapping turtles (*Myuchelys georgesi*). The infection was associated with necrotizing cystitis, nephritis, adenitis and vasculitis, and the presence of viral RNA in many tissues, indicating systemic spread of the virus (12). The target cell spectrum of serpentoviruses includes the epithelium of the respiratory tract and lungs (6), and in some cases also the oral cavity and the cranial esophagus (5–7, 11), the mucosa of which exhibits ciliated epithelium in snakes (13). Thus far, little is known about the intra- and interspecies transmission of serpentoviruses. However, recent studies demonstrated serpentovirus RNA in oral and cloacal swabs and the intestinal content of diseased and healthy snakes, suggesting that both airborne and fecal-oral transmission may occur (7, 9–11, 14).

In an earlier report, we studied the pathogenesis of serpentovirus-associated pneumonia in green tree pythons (6). Similar to other investigators who described serpentovirus pneumonia in pythons (5, 8, 10, 11), we occasionally detected the virus also in other organs, with and without evidence of pathological changes (6), suggesting that the cell tropism of python serpentoviruses goes beyond the respiratory epithelium. These findings and the fact that serpentovirus infections affect several python species led us to the hypothesis that serpentoviruses are not restricted to a certain species and have a broad disease potential. Therefore, we undertook a larger study, making use of diagnostic cases with natural serpentovirus infection. A total of 30 serpentovirus-infected snakes were selected based on demonstration of serpentovirus nucleoprotein (NP) by immunohistology in tissues with lesions. Seven python species from nine breeding colonies and collections were included, namely the green tree python (*Morelia viridis*), woma python (*Aspidites ramsayi*), carpet python (*Morelia spilota*), Angolan python (*Python anchietae*), ball python (*Python regius*), Indian python (*Python molurus*), and black-headed python (*Aspidites melanocephalus*). Immunohistology also helped to identify the serpentovirus target cells (6), and next-generation sequencing (NGS) served to obtain complete or near-complete genomes of the causative viruses. The results support the hypothesis that serpentovirus infections can cause variable disease in pythons, with lesions in a broad spectrum of tissues and organs and monocyte-mediated systemic spread of the virus.

RESULTS

Gross presentation of serpentovirus-associated disease in pythons. Full post-mortem examinations were performed on all cases. Most snakes that had died spontaneously exhibited the typical, previously described respiratory changes, represented by a varying amount of mucoïd material in the airways and particularly in the lungs (Fig. 1A). In some animals, the oral cavity, the trachea, the lung, and the air sacs were filled with mucoïd material, and the lung parenchyma appeared thickened (serpentovirus-associated proliferative disease; Fig. 1A); also, the mucoïd material was occasionally mixed with purulent exudate. Two euthanized carpet pythons with clinically reported

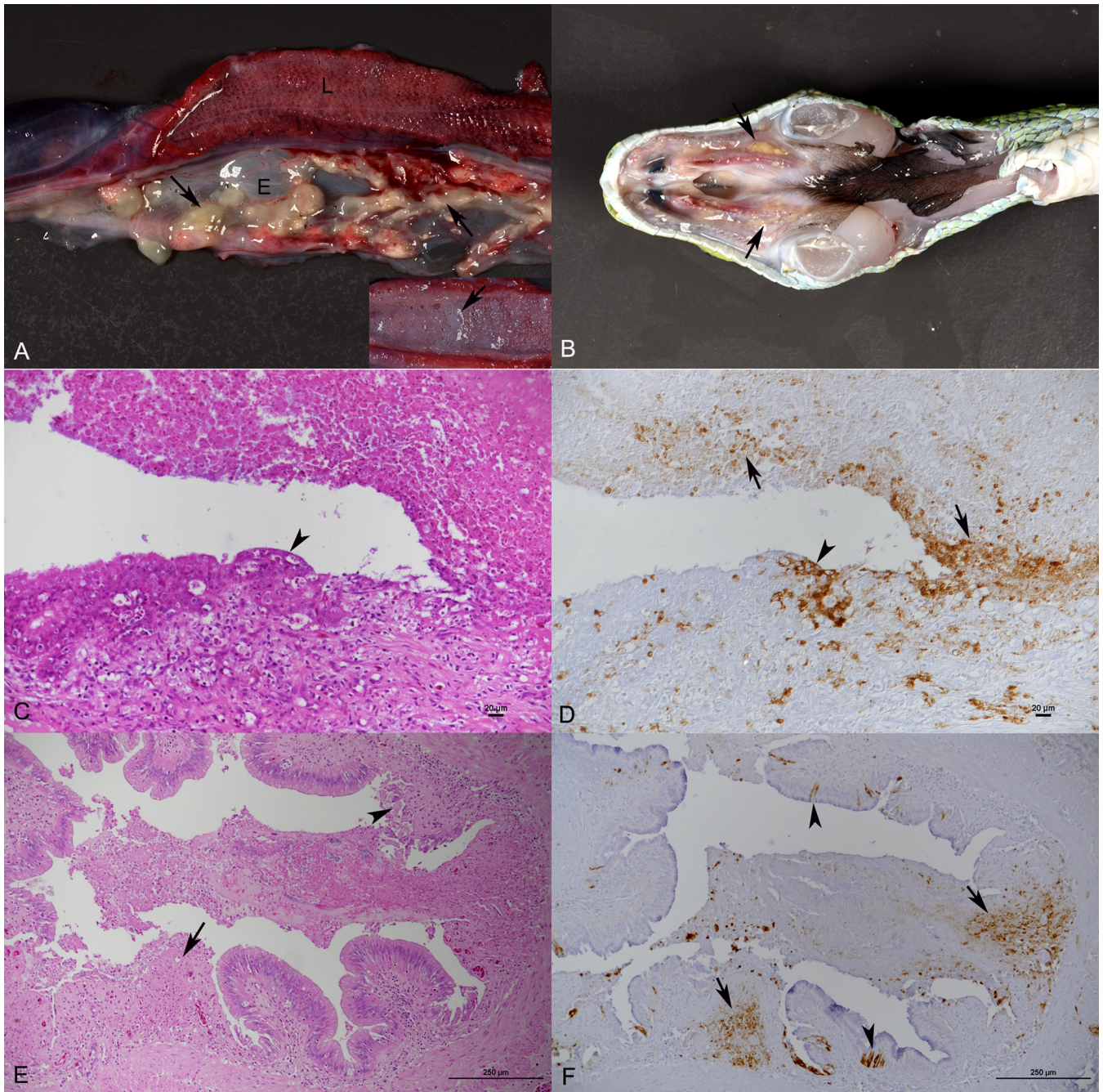


FIG 1 Serpentovirus disease. Lesions in the oral cavity and esophagus. (A and B) Snake CH-A8 (green tree python; *Morelia viridis*). (A) Lung (L) and esophagus (E). The lung appears voluminous and moist. The esophagus exhibits a severe multifocal fibrinonecrotic inflammation (arrow). (Inset) Lung after longitudinal section, with accumulation of abundant mucoid fluid in the lumen. (B) Oral cavity, ventral aspect. Focal fibrinonecrotic stomatitis (arrows). (C and D) Snake CH-A4 (Woma python; *Aspidites ramsayi*). Nasal mucosa. (C) Severe fibrinonecrotic rhinitis. There is extensive serpentine necrosis (arrows) and NP expression (arrowheads). (D) Both cell-free in areas of necrosis (arrows) and within epithelial cells (arrowheads). Bars = 20 μ m. (E and F) Snake CH-A7 (green tree python; *Morelia viridis*). Esophagus. (E) Severe multifocal fibrinonecrotic esophagitis. Serpentovirus NP expression is seen both cell-free in areas of necrosis (arrows) and within infected epithelial cells (arrowheads). Bars = 250 μ m. (C and E) HE stain. (D and F) Immunohistology, hemalaun counterstain.

respiratory distress (CH-B1 and -B2; Table 1) did not exhibit any gross pulmonary changes but showed mild mucus accumulation in the oral cavity. In others, granulomatous and/or fibrinonecrotic lesions were observed in the oral, esophageal, and intestinal mucosa (Fig. 1A and B, 2A and B), in liver (Fig. 3A), spleen, or kidney, the coelomic cavity, and the oviduct. There was no evidence of a specific lesion pattern in the different affected python species; the findings for each animal are summarized in Table 1.

TABLE 1 Animals, clinical signs, lesions, and viral target cells^{a,b}

Animal	Species	Age	Sex	Clinical history	Lesions (affected tissues) ^c	Viral target cells ^d	Virus detection ^e
CH-A1 ^f	<i>Morelia viridis</i>	8 yr	M	RD, mucus in OC	NPD (NC, T, L), FNI (Sp, Es)	EP (NC, OC, T, L, R, Es)	PCR (L)
CH-A2	<i>Morelia viridis</i>	5 yr	M	RD	NPD (T, L)	EP (T, L)	PCR (L)
CH-A3	<i>Morelia viridis</i>	2 yr	M	RD	NPD (NC, OC, L)	EP (NC, OC, L)	PCR (L)
CH-A4	<i>Aspidites ramsayi</i>	3 mo	NK	RD, mucus in OC	NPD (NC, OC, L)	EP (NC, OC, L)	PCR (L), NGS (SNT)
CH-A5	<i>Morelia spilota</i>	4 yr	F	No history	NPD (NC, OC, T, L)	EP (NC, OC, T, L)	PCR (L), NGS (SNT)
CH-A6	<i>Morelia spilota</i>	1 yr	M	RD	NPD (T, L)	EP (T, L)	PCR (Ch, CI)
CH-A7	<i>Morelia viridis</i>	Adult	F	Sudden death	NPD (NC, OC, T), FNI (Th, Sp), V (He, Sp, Si), SGD (He, Es, Si)	EP (NC, OC, T, L, RT, Li, PD, E, Es, Si), macrophages	PCR (L), NGS (SNT, liver)
CH-A8	<i>Morelia viridis</i>	1.5 yr	M	Sudden death	NPD (NC, OC, T), SGD (Es, Si, Li, LIV, Sp)	EP (NC, OC, T, L, RT, Hep, PD), VE, macrophages, monocytes	NGS (SNT, L, liver)
CH-A9	<i>Python regius</i>	Adult	NK	No history	NPD (NC, OC, T), FNI (Es)	EP (NC, OC, T, L, Es, RT)	PCR (L, Ch, CI)
CH-B1	<i>Morelia spilota</i>	1 yr	M	RD	NPD (NC, OC), FNI (K)	EP (NC, OC, T, L, PD, RT)	PCR (L, CI), NGS (SNT)
CH-B2	<i>Morelia spilota</i>	1 yr	M	RD	NPD (NC)	EP (NC)	PCR (L)
CH-B3	<i>Morelia viridis</i>	NK	M	RD	NPD (T, L), FNI (K, P)	EP (L, PD, RT)	PCR (L, Ch, CI), NGS (SNT)
CH-B4	<i>Morelia spilota</i>	1 yr	M	RD	NPD (NC, OC, T, L)	EP (NC, OC, T, L)	PCR (L, Ch)
CH-B5 ^f	<i>Python anchietae</i>	8 yr	M	RD	NPD (T, L)	EP (NC, OC, T, L)	NGS (SNT)
CH-B6	<i>Morelia viridis</i>	1.5 yr	M	Sudden death	NPD (NC, OC, T), FNI (Es, Si, Li, Sp), SGD (Es, Si, Li, Th, K, He, LIV), V (Th, He)	EP (NC, OC, T, L, RT, Es, S, PD, Hep); ependyma	PCR (L, K), NGS (liver)
CH-C1	<i>Morelia viridis</i>	Adult	F	RD	NPD (OC, T, L), SGD (R)	EP (NC, OC, T, L, RT)	PCR (Ch, CI)
CH-C2 ^f	<i>Morelia spilota</i>	6 yr	F	RD	NPD (NC, OC, T, L)	EP (NC, OC, T, L)	PCR (L)
CH-C3	<i>Morelia viridis</i>	Juv	F	Sudden death	SGD (L, LIV, K, Si, Li), FNI (Es, M), V (Si, Li)	EP (L, RT, Hep, Es, Si, Li, M), VE, macrophages, monocytes	NGS (SNT, liver)
CH-C4	<i>Aspidites melanocephalus</i>	Adult	M	Anorexia	NPD (T, L), FNI (Es)	EP (T, L, Es)	PCR (L, Ch, CI)
CH-D1	<i>Python regius</i>	NK	M	RD	NPD (NC, OC, T, L), FNI (Es)	EP (T, L, Es)	PCR (L, Ch, CI)
CH-D2	<i>Python regius</i>	NK	M	RD	NPD (NC, OC, T, L), FNI (Es)	EP (T, L, Es)	PCR (L, Ch, CI), NGS (SNT)
CH-E2	<i>Python regius</i>	NK	F	RD	NPD (T, L), FNI (Es)	EP (T, L, Es)	PCR (L, Ch, CI), NGS (SNT)
CH-F1	<i>Morelia viridis</i>	10 yr	F	No history	NPD (NC, OC, T, L), FNI (M, Si, Li), V (Ov), SGD (LIV, Ov)	EP (NC, OC, T, L, Hep, RT, Si, Li, PD, Ov) VE, ependyma, macrophages, monocytes	PCR (L), NGS (SNT)
CH-F2	<i>Morelia viridis</i>	6 yr	F	Anorexia	NPD (NC, OC, T, L)	EP (NC, OC, T, L, Es, PD)	PCR (L), NGS (L, SNT)
E-A1	<i>Python regius</i>	NK	NK	No history	NPD (L)	EP (L)	
E-A2	<i>Python anchietae</i>	NK	NK	Sudden death	NPD (T, L)	EP (T, L)	PCR (L)
E-B1	<i>Python regius</i>	Juv	M	RD, mucus in OC, anorexia	NPD (T)	EP (T, L, PD)	PCR (L)
E-B2 ^g	<i>Python regius</i>	1 yr	M	RD, mucus in OC	NPD (NC, OC, T, L)	EP (T, L)	PCR (L), NGS (SNT)
E-B3	<i>Python regius</i>	Juv	M	RD, mucus in OC	NPD (L)	EP (T, L)	PCR (L), NGS (SNT)
E-C1	<i>Morelia viridis</i>	4–5 yr	M	No history	NPD (NC, OC, T, L)	NE	PCR (L), NGS (SNT)

^aAll animals were from breeding collections in Switzerland (CH) or Spain (E). Breeders CH A-C and CH-F were working closely together, trading/exchanging snakes.

^bM, male; F, female; OC, oral cavity; NC, nasal cavity; T, trachea; L, lung; He, heart; Es, esophagus; S, stomach; Si, small intestine; Li, large intestine; LIV, liver; K, kidney; Th, thymus; Sp, spleen; Ov, oviduct; M, mesothelium; PD, pancreatic ducts; RT, renal tubules; EP, epithelial cells; PD, pancreatic duct epithelia; VE, vascular endothelial cells; Hep, hepatocytes; NK, not known; juv, juvenile; RD, respiratory distress; nk, not known.

^cNPD, nidovirus-associated proliferative disease (with variable degree of epithelial hyperplasia and inflammation); FNI, fibrinonecrotizing inflammation; SGD, systemic granulomatous disease; V, vasculitis and perivasculitis.

^dViral antigen expression in cells (detected by immunohistology) with or without evidence of cytopathic effect.

^eIn all animals, nidovirus-associated disease was confirmed by immunohistology, confirming the presence of virus within the lesions. In addition, RT-PCR for nidovirus (PCR) was performed on tissue samples and/or cloacal (CI) and choanal (Ch) swabs (6), or next-generation sequencing (NGS) was performed on culture supernatants from *Morelia viridis* cell cultures (6) incubated with lung homogenates (SNT) or from liver tissue (liver).

^fRoutine bacteriological examination was performed on lung samples, with the following results: CH-A1, *Pseudomonas aeruginosa*, *Proteus* sp., *Citrobacter braakii*; CH-B5, negative; CH-C2, *Pseudomonas aeruginosa*, *Providencia rettgeri*.

^gRoutine virological examination for adenovirus, arenavirus, paramyxovirus, ferlavirus, and reovirus was performed in a commercial laboratory on a lung sample, with negative results.

Serpentoviruses have a broad target cell and lesion spectrum. From all animals, the major organs and tissues as well as gross lesions were studied by histology and immunohistology for serpentovirus NP. The examination revealed a broad target cell spectrum and serpentovirus-associated cytopathic effect.

Oral cavity and respiratory tract. The respiratory tract was found to be affected in all animals (100%), with a variable distribution of viral infection and lesions. In 10 animals (33%), the nasal and oral cavities were affected and exhibited multifocal extensive epithelial necrosis with diffuse subepithelial infiltration of the adjacent, partly hyperplastic respiratory and squamous epithelium by numerous heterophils, lymphocytes, plasma cells, and macrophages. Lesions were occasionally covered with fibrin, degenerated epithelial cells, and heterophils (fibrinonecrotic rhinitis and stomatitis; Fig. 1C). Serpentovirus NP was abundantly expressed in numerous unaltered and

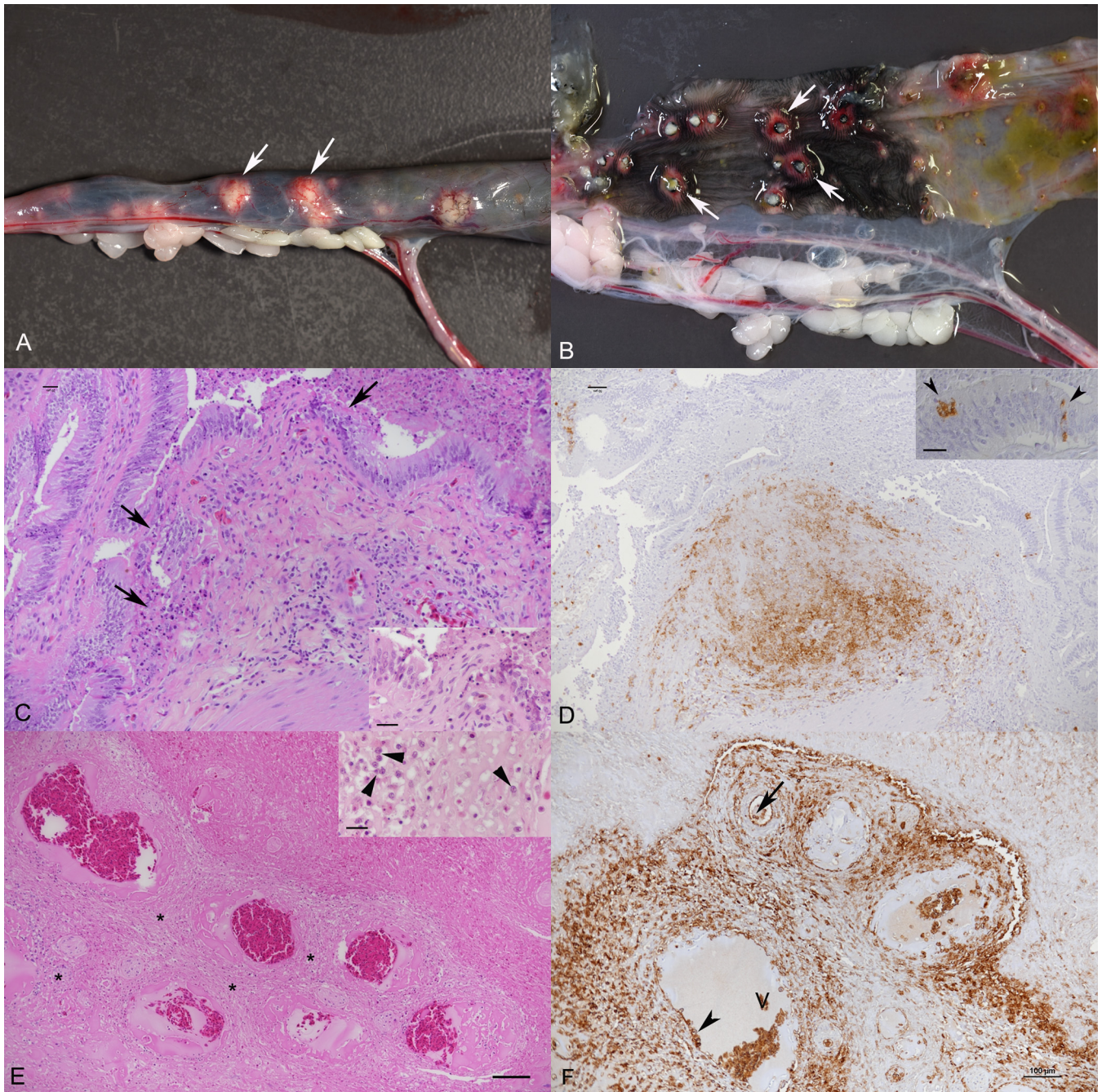


FIG 2 Serpentovirus disease. Intestinal lesions. (A and B) Snake CH-B6 (green tree python; *Morelia viridis*). Severe multifocal fibrinonecrotic enteritis with ulcerations (arrows). (C and D) Snake CH-C3 (green tree python; *M. viridis*). Small intestine. (C) Severe focal pyogranulomatous perivascular infiltrates and superficial fibrinonecrotic inflammation (arrows, inset). (D) Serpentovirus NP is abundantly expressed within pyogranulomatous infiltrates. (Inset) Intact infected enterocytes adjacent to the ulceration (arrows). (E and F) Snake CH-A7 (green tree python; *M. viridis*). (E) Large intestine, submucosa. Severe pyogranulomatous perivascular infiltrates (inset: abundant macrophages [arrowheads] in the infiltrate) with extensive serpentovirus NP expression (F) within inflammatory infiltrates and within intravascular leukocytes and vascular endothelial cells (arrowheads). V, vein. (C and E) HE stain; (D and F) immunohistochemistry, hemalaun counterstain. (C) Bar = 20 μm . (D) Bar = 50 μm ; (inset) bar = 20 μm . (E and F) Bars = 100 μm ; (inset) bar = 20 μm .

degenerated oral and nasal epithelial cells (Fig. 1D). In two euthanized carpet pythons (CH-B1 and -B2; Table 1), these were the only pathological changes, suggesting that they represented early (initial) lesions. The latter is further supported by the fact that in one of the two individuals (CH-B1), serpentovirus NP was also detected in a few individual respiratory epithelial cells in the trachea, some trabecular pseudostratified lung epithelial cells, and occasional type I pneumocytes lining the faveolar space (Fig.

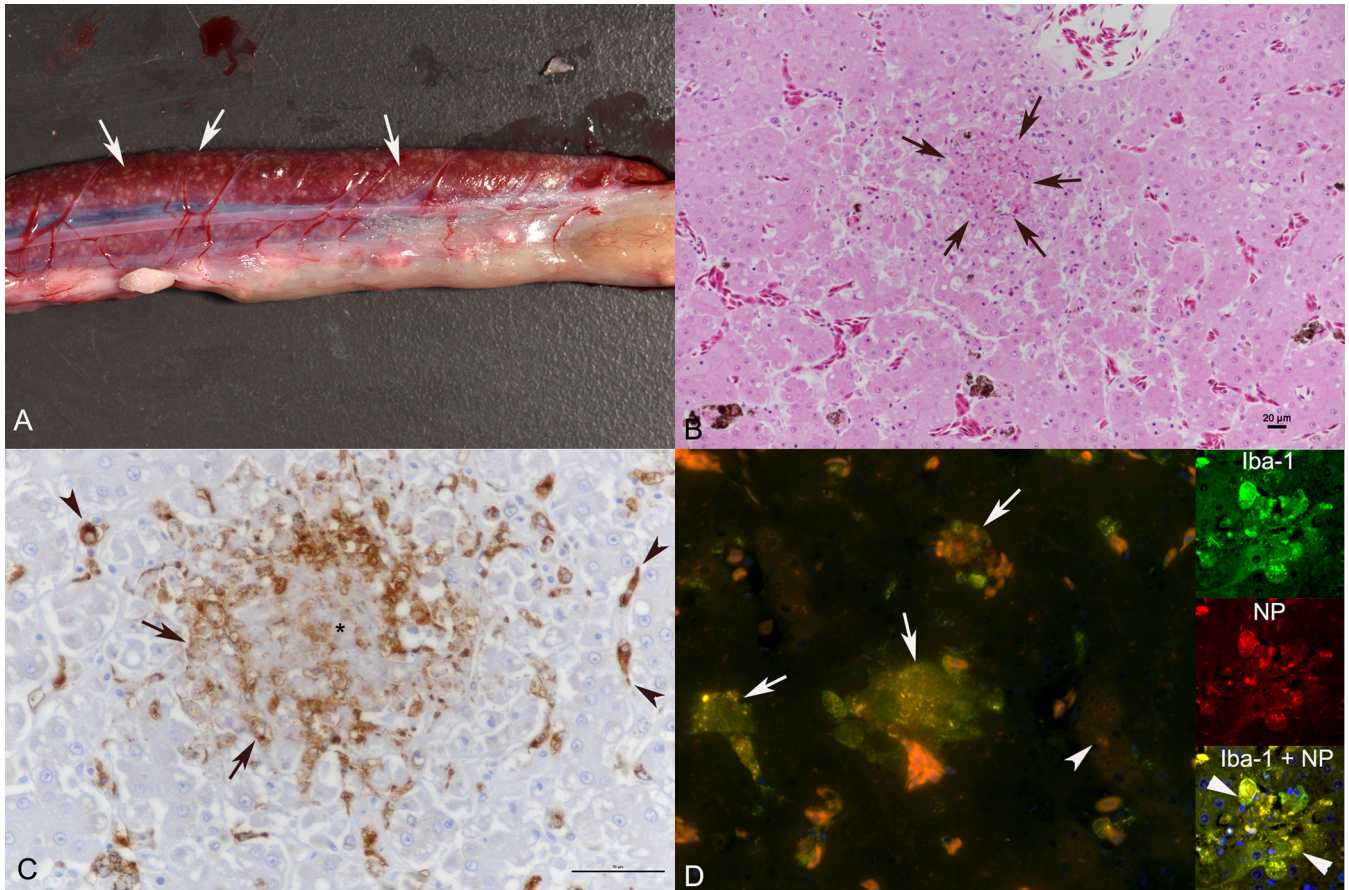


FIG 3 Serpentovirus disease. Involvement of the liver. (A) Snake CH-B6 (green tree python; *Morelia viridis*). Severe multifocal pyogranulomatous hepatitis (arrows). (B to D) Snake CH-C3 (green tree python; *M. viridis*). (B) Focal granuloma (arrows). HE stain. Bar = 20 μm . (C) Closer view of granuloma, with central area of necrosis (asterisk), surrounded by numerous macrophages that exhibit strong serpentovirus NP expression (arrows). Viral antigen expression is also seen in Kupffer cells (arrowheads). Immunohistology, hemalaun counterstain. Bar = 50 μm . (D) Double immunofluorescence of a granuloma confirms serpentovirus NP expression (red) within macrophages (Iba-1+; green; arrows). There is also a hepatocyte with weak serpentovirus NP expression (arrowhead). The column of insets on the right shows another small granuloma highlighting NP-positive macrophages (arrowheads).

4A), without evidence of cell damage or inflammation. Two ball pythons with fibrinonecrotic rhinitis and stomatitis (E-B1 and -B3) also exhibited a diffuse chronic tracheitis with subepithelial infiltration by lymphocytes, plasma cells, macrophages, and occasional heterophils, but no further lesions in the lower respiratory tract.

The remaining snakes showed histological evidence of serpentovirus-associated proliferative disease with epithelial hyperplasia in the nasal cavity, trachea, and lung, as well as mucus and inflammatory cells filling the faveolar space, consistent with our earlier findings (6). Serpentovirus NP expression was seen in the pseudostratified epithelium of the primary trabeculae and in type I and type II pneumocytes of the faveolar space; the extent and distribution varied between animals.

Alimentary tract. In addition to the respiratory changes, several individuals (CH-A1 and -A9, CH-B6, CH-D1 and -D2, CH-C4, and CH-E; carpet pythons, green tree pythons, ball pythons, and a black-headed python) exhibited a severe multifocal fibrinonecrotic esophagitis (Fig. 1E and F) with abundant serpentovirus-infected intact and degenerate squamous epithelial cells. The gross intestinal lesions observed in another four cases (CH-A7 and -A8, CH-B6, CH-F1) were indeed serpentovirus induced, since all exhibited a multifocal fibrinonecrotic enteritis with serpentovirus NP expression in individual intact and degenerating enterocytes (Fig. 2C and D).

Vascular involvement, systemic spread, and systemic granulomatous and/or fibrinonecrotic disease. In all snakes with the above-described intestinal changes (CH-A7 and -A8, CH-B6, CH-F1), the mucosal lesions were found to overlie focal

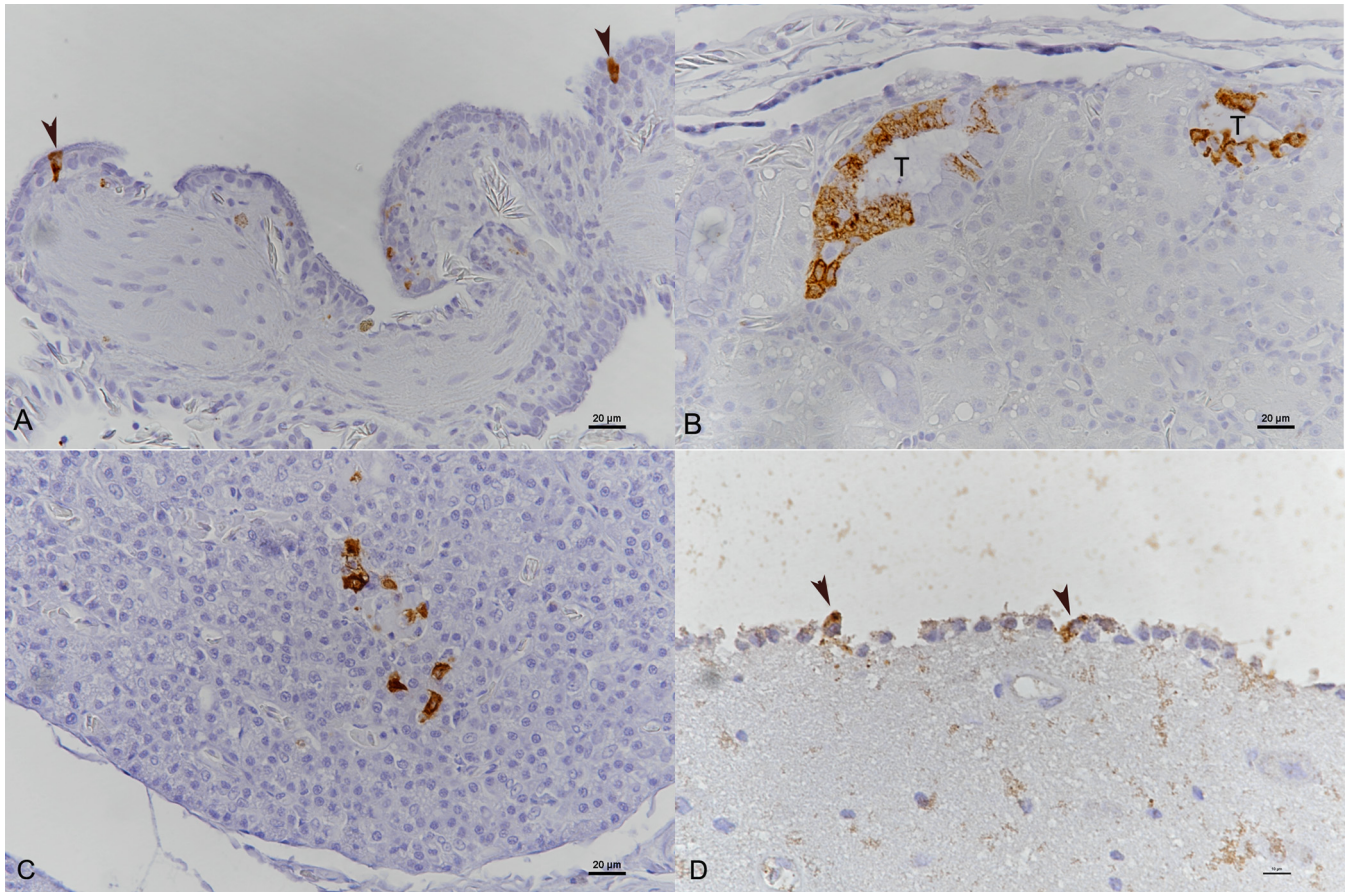


FIG 4 Serpentovirus disease. Serpentovirus NP expression in various types of epithelial cells. (A) Snake CH-B1. Lung (carpet python; *Morelia spilota*). Positive respiratory epithelial cells (arrowheads). (B and C) Snake CH-B3 (green tree python; *Morelia viridis*). (B) Kidney. Positive tubular epithelial cells. T, tubular lumen. (C) Pancreas. Serpentovirus NP expression in pancreatic duct epithelial cells. (D) Snake CH-F1 (green tree python; *M. viridis*). Brain. Positive ependymal cells lining the ventricle. Immunohistoology, hemalaun counterstain. (A to C) Bars = 20 μ m. (D) Bar = 10 μ m.

inflammatory processes in the intestinal wall. These were represented by multifocal (pyo)granulomatous perivascular infiltrates of macrophages and fewer heterophils and lymphocytes, which were predominantly seen in the submucosa in close proximity to the gut-associated lymphatic tissue (GALT) but occasionally extended into the tunica muscularis (Fig. 2C and E). These lesions contained abundant serpentovirus NP in infiltrating macrophages (Fig. 2D and F). Occasional affected vessels also exhibited fibrinoid degeneration of the wall with intramural heterophil infiltration. A multifocal pyogranulomatous vasculitis and perivascularitis of small, medium-sized, and large veins and arteries was also seen in the serosa of various organs, e.g., the heart, the lung, and the thymus, of four snakes (CH-A7, CH-B6, CH-C3, CH-F1) (Fig. 5C and D). Here, serpentovirus NP was detected not only in macrophages of the infiltrates, but also in endothelial cells, which often appeared to be activated (Fig. 2F), and in mononuclear cells in the vessel lumina (Fig. 2F and 4A). Staining for the monocyte/macrophage marker Iba-1 showed that the mononuclear cells in the vessel lumina were predominantly Iba-1 positive, i.e., monocytes (Fig. 5B). The latter finding suggests monocyte-associated viremia and viral spread via infected monocytes.

Interestingly, all animals with the described vascular lesions were green tree pythons (CH-A7, CH-B6, CH-C3, CH-F1) and also exhibited multifocal pyogranulomatous lesions, which consisted of a central area of necrosis, surrounded by virus-laden macrophages (Fig. 5C and D). Affected organs included the kidneys, thymus, heart, and liver, and in one animal (CH-C3), the lung. One green tree python (CH-F1) also exhibited pyogranulomatous and fibrinonecrotic lesions in the oviduct, with serpentovirus NP

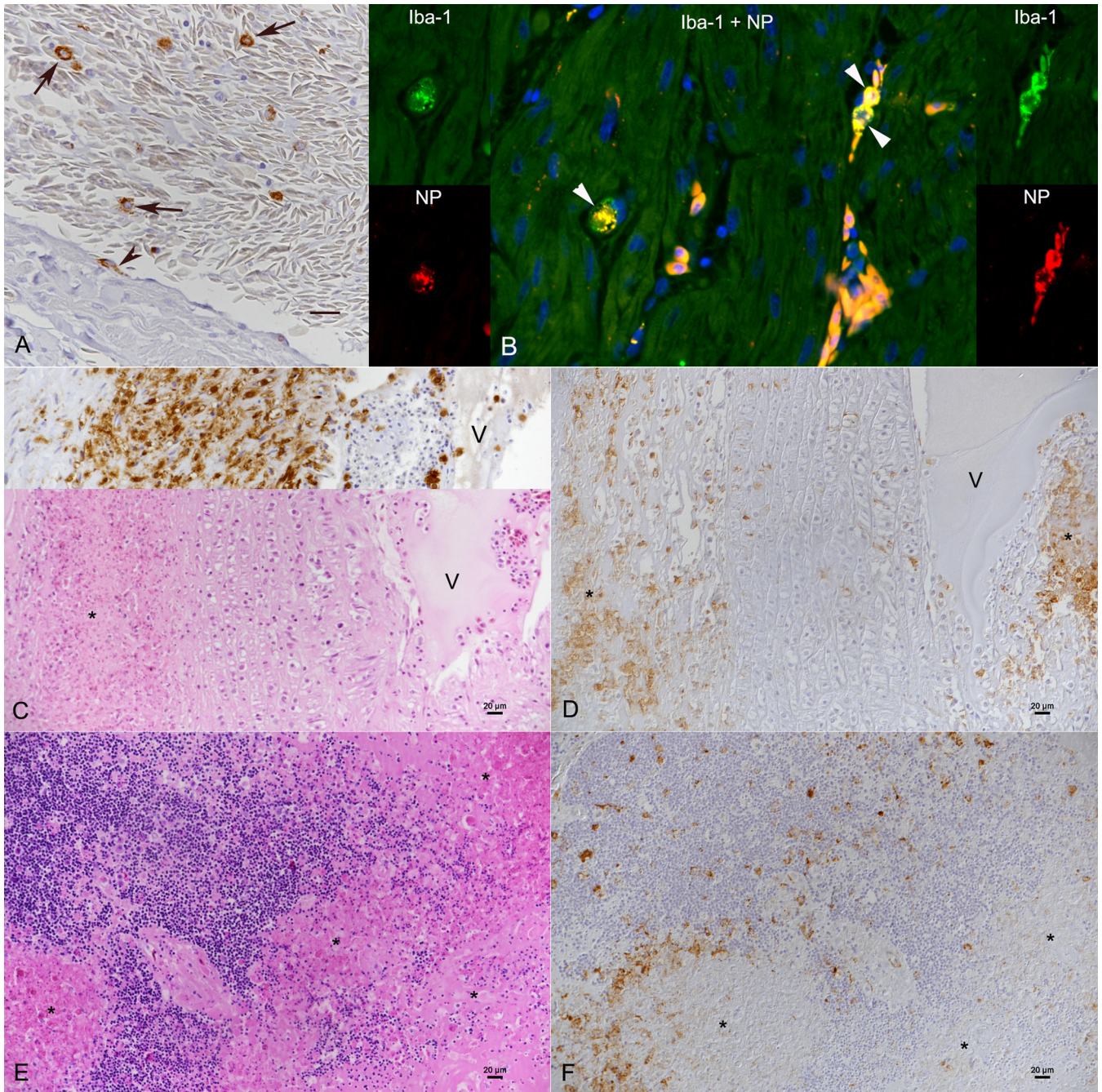


FIG 5 Serpentovirus disease. Involvement of blood vessels and monocyte-associated viremia. (A and B) Snake CH-C3 (green tree python; *M. viridis*). (A) Lung, blood vessel. Serpentovirus NP expression is seen in circulating monocytes (arrows) and individual endothelial cells (arrowhead). Immunohistochemistry, hemalaun counterstain. (B) Myocardium, capillaries. Double immunofluorescence confirms serpentovirus NP expression (red) in monocytes (Iba-1+; green). NP, The orange fluorescence seen in the abundant oval-shaped cells represents autofluorescence of erythrocytes. (C and D) Snake CH-A7 (green tree python; *M. viridis*). Lung, serosal artery. (C) Mild transmurular mononuclear infiltration and marked granulomatous to necrotizing perivascular infiltration (asterisk; inset: staining for Iba-1 confirms that the infiltrating cells are predominantly macrophages) with abundant serpentovirus NP expression (D) within infiltrating cells. V, vessel lumen. Bars = 20 μm. (E and F) Snake CH-B6 (green tree python; *M. viridis*). Thymus. (E) Focal areas of necrosis (asterisks), surrounded by abundant serpentovirus NP-positive macrophages. Serpentovirus NP expression is also seen cell-free within areas of necrosis. Bars = 20 μm. (C [inset], D, and F) Immunohistochemistry, hemalaun counterstain.

found cell-free in necrotic debris. This was seen together with a fibrinous coelomitis in the caudal coelomic cavity, adjacent to the inflamed oviduct. Pyogranulomatous lesions varied in distribution and extent between individuals but were always present in more than one organ. There was no histological evidence of bacteria within the lesions.

Animals with pyogranulomatous lesions often showed serpentovirus NP in epithelia adjacent to the inflammatory foci (e.g., pancreatic ducts, renal tubules, etc.) without any evidence of degeneration or necrosis (Fig. 4B and C).

Overall, fibrinonecrotic lesions were observed in five green tree pythons (CH-A1 and -A7, CH-B6, CH-C3, CH-F1) and one carpet python (CH-B1). They were represented by diffuse necrosis and fibrin exudation in parenchymatous organs (spleen, thymus) or on the serosal surface of the coelomic cavity (in close proximity to affected organs) with minimal inflammatory response (Fig. 5E and F). These lesions were often observed in animals with serpentovirus-associated perivascular/vascular and/or pyogranulomatous lesions, indicating massive systemic spread of the virus.

Infection of epithelial cells and ependyma. As described, serpentovirus NP was detected in various types of epithelial cells, often in close proximity to granulomatous or fibrinonecrotic lesions and without evidence of cell degeneration or necrosis. Affected epithelial cells included type I and type II pneumocytes of the lung, epithelial cells of renal tubules and pancreatic ducts, mesothelial cells (Fig. 4A to C), and hepatocytes (Fig. 3D). In two cases (CH-B6 and -F1), ependymal cells were also found to be infected, without evidence of correlating brain lesions (Fig. 4D).

Virus isolation and identification. Serpentovirus isolation was attempted by inoculating primary cell cultures of green tree python fetal liver and brain tissue with lung tissue homogenates of 24 animals that had been confirmed as serpentovirus infected by immunohistology and RT-PCR. After inoculation, cytopathic effects were observed in 12/24 samples at about 3 to 4 days postinfection (dpi). Initial changes included enlargement, rounding, and cytoplasmic vacuolization of cells. This was followed by progressive loss of adherence and detachment from 3 dpi onward. Two serpentovirus-positive lung specimens (CH-A8, CH-F2; Table 1), three positive liver specimens (CH-A7 and -A8 and CH-B6; Table 1), a lung lavage sample, and 16 cell culture supernatants (Table 1) were subjected to NGS. To investigate if the viruses were of the same species, we included samples from both the Swiss and Spanish collections. The approach yielded serpentovirus sequences from 14 lung culture supernatants. *De novo* genome assembly from tissue sample after removal of reads matching the host's genome produced contigs covering the complete coding sequence (CDS) of a novel serpentovirus in Switzerland. The genome organization of the identified serpentovirus was identical to those described for Ball python nidovirus (BPNV) and *Morelia viridis* nidovirus (MVNV). The open reading frame 1b (ORF1b, RNA-dependent RNA polymerase) of these viruses had less than 5% nucleotide and less than 2.4% amino acid differences with recently described MVNV isolates BH128 14-12 and BH171 14-7 and *Serpentovirinae* sp. isolates L3, L4, and H0-1 but more than 13% nucleotide and 8.5% amino acid differences to all other serpentovirus strains. Phylogenetic analysis based on ORF1b suggested that this virus forms a sister clade to the previously known python-associated serpentovirus species, BPNV and MVNV (Fig. 6). CDSs of the same virus species were obtained from 11 cell culture supernatants, including the isolation attempts from the liver samples included in the NGS analysis. One of the cell culture supernatants analyzed by NGS yielded CDS of MVNV (animal E-C1; Table 1), and for four cell culture supernatants, NGS failed due to severe bacterial contamination.

For three snakes (CH-A7, -A8, CH-C3; Table 1), the analysis included cell culture-isolated virus (lung homogenate as inoculum) and virus sequenced directly from tissue (liver). The consensus sequences obtained from liver tissue and the respective cell culture isolate were identical for each of these three snakes, indicating that isolation did not induce a marked bias in the sequence analysis. Single nucleotide variant (SNV) analysis of the NGS data did not show evidence of significant differences in the sequences obtained from different organs or from cell culture isolates. Likewise, the SNV analysis did not find differences between the viral populations obtained from animals with or without systemic infection, suggesting that viral intrahost polymorphism does not explain the varying pathogenic manifestation. However, to confirm this

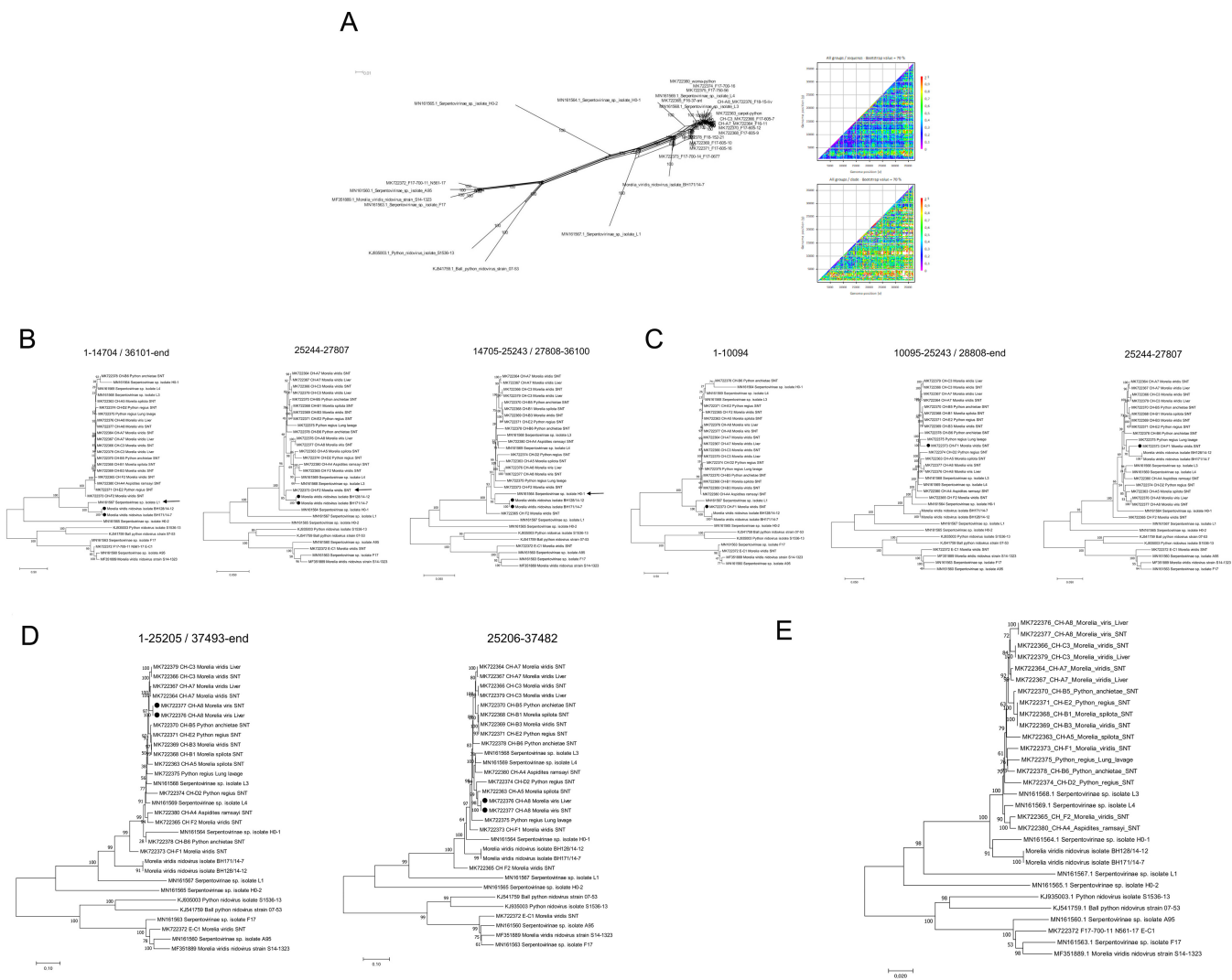


FIG 7 Recombination analysis of serpentovirus genomes. (A) Phylogenetic network and tree order scan showed evidence of recombination in the sequence data set. (B to D) Incongruent tree topologies of virus strains with highly supported recombination events estimated using RDP software. The numbers above trees show the genome regions in alignment. (E) Phylogenetic tree based on concatenated nonrecombinant genome regions.

BH128/14-12, and strain CH-F1) cluster together in the 5' end of the genome, the genetic distances between these strains are rather high in this region, suggesting that the exact recombination partners are not represented in the data set. Since *Serpentovirinae* sp. isolate L1 was sequenced from a *Python regius* in the United States in 2015 (14), whereas the strains BH171/14-7, BH128/14-12 (15), and CH-F1 were isolated from a *Morelia viridis* in Germany (2015) and in Switzerland (2018), it is likely that the recombination events have occurred between the ancestors of these lineages.

Another clear recombination event was detected in the strain CH-A8 (MK722376), which clusters together with the strains CH-A7 and CH-C3 based on the majority of the genome, whereas between nucleotides 25205 and 37482, it clusters with CH-A5 (MK722363) (Fig. 7D). In addition, the strain CH-D2 clusters together with this group (CH-A8/CH-A5) based on nucleotides 25205 to 37482.

Sequential exclusion of recombinant regions from the alignment (i.e., nucleotides 1 to 14704 and 25144 to 37869) resulted in the tree shown in Fig. 7E. Although some of the methods included in RDP4 analysis still found evidence of recombination in this alignment, the further removal of these regions did not affect the topology of the tree.

The phylogenetic tree indicated that multiple viral strains circulate among the snakes of a single breeder, and on the other hand, there are some indications of viral

transmission between the breeders, as exemplified by the high similarity of strains CH-B1, CH-B3 (breeder CH-B) and CH-E2 (breeder CH-E). Breeders CH-A, CH-B, CH-C, and CH-F exchanged animals, which may explain the grouping of strains CH-C3, CH-A7, CH-B1, CH-B3, CH-B5, and CH-A8 to a single cluster.

Evidence of horizontal transmission within colonies and of virus shedding from diseased animals. One Swiss breeder (CH-B; Table 1) lost one of three juvenile carpet pythons from the same clutch that had been housed separate from each other but in the same room (distance less than 0.5 m) to severe fatal proliferative pneumonia (CH-B4). The postmortem examination confirmed serpentovirus-associated pneumonia in the deceased animal, prompting the breeder to submit the two siblings (CH-B1 and -B2; Table 1) for euthanasia and diagnostic postmortem examination. Both individuals exhibited serpentovirus-associated lesions in the upper airways but not in the lung, suggesting that these cases represented an early disease stage.

In addition to the above-described snakes, we studied choanal and/or cloacal swabs from seven additional animals from different collections for the presence of serpentovirus RNA by RT-PCR. All of the tested animals were found positive for serpentovirus infection (Table 1) and included individuals with serpentovirus-associated proliferative disease (respiratory form) and individuals with evidence of granulomatous and fibrinonecrotic disease (systemic form), supporting results from previous studies that animals shed the virus (8, 14). Further, the virus strains from snakes CH-B1, CH-B3, and CH-B5 showed high genetic identities and clustered together in the phylogenetic trees, suggesting viral transmission between the snakes of breeder CH-B.

Pathological changes unrelated to serpentovirus infection. Individual snakes exhibited additional lesions that appeared to be unrelated to serpentovirus infection, as confirmed by immunohistology for serpentovirus NP, renal gout (CH-A3 and E-A1; Table 1), and a necrotizing splenitis (CH-A1 and CH-C4; Table 1) and fibrinonecrotic enteritis with intralesional coccoid bacterial colonies (E-B1; Table 1). Both conditions are likely a consequence of debilitation/dehydration due to chronic pulmonary disease.

DISCUSSION

Serpentoviruses have recently been described as the cause of respiratory tract disease in several python species in the United States and Europe (5, 6, 10, 11), representing an emerging threat to python traders and breeders in particular. The present study aimed to further elucidate the potential species specificity of and/or susceptibility to serpentoviruses, their phylogeny and geographic divergence, as well as viral shedding and transmission, host cell tropism, and type of associated disease, focusing on natural cases from different geographic regions and breeding colonies.

Pythons are nonvenomous snakes found in Africa, Asia, and Australia. The present study shows that python species originating from all three continents are susceptible to serpentoviruses, confirming previous studies (5, 6, 8, 10, 11, 14, 15); indeed, they can develop serpentovirus-associated disease.

In our study, no differences were noted between the various python species in the degree and distribution of serpentovirus-associated respiratory disease. However, it is interesting to note that all animals with systemic viral spread (indicated by disseminated granulomatous and/or fibrinonecrotic lesions, [peri]vascular lesions, infected monocytes, etc.) were of the genus *Morelia*. Anecdotal information from the breeders suggests that breeding *M. viridis* is considered challenging, as they require a high level of humidity in their natural habitat (up to 90% to 100%), which is difficult to maintain in captivity. Our results suggest increased susceptibility of this genus to serpentovirus infection and/or disease, a finding also supported by recent epidemiologic studies (14). In support, the SNV analysis of the viral genomes did not reveal nucleotide differences in the viral genome that would associate with the differences in the disease manifestation. However, functional experiments such as experimental infection with infectious clones would be needed in order to draw firm conclusions.

Recently, experimental infection of ball pythons established the causal relationship between serpentovirus infection and inflammation with excess mucus production of

the upper respiratory and the gastrointestinal tract as the main pathological process early, i.e., within the first 12 weeks, after infection (7). Infected pythons showed severe respiratory distress with only minimal pneumonia, most likely because the mucus overproduction resulted in obstruction of the upper airways (7). These findings correlate with those we made when studying naturally infected cases; some animals were submitted for euthanasia due to acute respiratory distress but only exhibited inflammatory processes in the nasal and oral cavity, without histologic evidence of tracheitis or pneumonia. In all other naturally infected animals, rhinitis, stomatitis, and tracheitis were present, as well as a variable degree of proliferative pneumonia, indicating longer duration and a more progressed stage of the disease. On that note, the anatomic structure of the snake lung has to be considered, as studies on Burmese pythons have shown that python lungs provide excess capacity for oxygen exchange. This leads to progressive spread of respiratory infections through the lung, thereby continuously reducing respiratory gas exchange without causing clinical signs. The latter will develop only when the oxygen exchange capacity falls below the requirements of the metabolic rate. This is particularly relevant in association with hyperplasia of the pulmonary epithelium, which has an impact on the blood gas exchange (16). In some snakes, we additionally observed an esophagitis; this is interpreted as a consequence of overspill and swallowing of virus-laden mucus, a theory also supported by previous studies (6, 7, 16). The esophageal epithelium contains ciliated cells in various snake species (13), which represent the primary site of viral replication in human coronaviruses (17).

Similar to serpentoviruses, mammalian toroviruses (found in horses, swine, and cattle) belong to the family *Tobaniviridae* and seem to show a high seroprevalence in affected populations. For example, the seroprevalence to porcine torovirus (PToV) exceeds 95% in swine populations, (18) and is 94% in cattle (Breda virus) (19) and 38% in horses (Berne virus) (20). Equine and porcine toroviruses are generally associated with asymptomatic enteric infections, and transmission is probably via the oral/nasal route through contact with feces (21) or nasopharyngeal secretions (22).

In our study, serpentovirus RNA was detected in choanal and cloacal swabs of individuals presenting with either the respiratory (local) or systemic form of the disease. This correlates with studies on human coronaviruses (Middle East respiratory syndrome coronavirus [MERS-CoV] and severe acute respiratory syndrome coronavirus-2 [SARS-CoV-2]), where viral RNA was detected not only in throat swabs but also in stool samples (23, 24). Viral shedding via the feces in pythons without intestinal lesions could likely be a consequence of the swallowing of mucus. Therefore, besides the respiratory (aerosol) route, the fecal-oral route also appears to be a likely way of transmission in pythons, a claim supported by previous studies (7, 8, 10, 15). The literature suggests that mammalian coronaviruses have a limited host cell tropism and affect either the intestinal or the alveolar epithelium (6, 7, 10, 11, 22, 25–27). This seems not to apply to serpentoviruses, for which the results of the present study indicate a rather broad cell tropism, for various types of epithelia (respiratory and pulmonary epithelium, enterocytes, hepatocytes, epithelial cells in renal tubules and pancreatic ducts) and ependymal cells. Interestingly, a similar tendency is described for SARS CoV and SARS-CoV-2, whose broad cell tropism also includes infection of endothelial cells (28, 29), as also shown for serpentoviruses in the present study. Serpentovirus RNA has previously been detected in several tissues of affected snakes (10), but only the present study detected the various cell types targeted by the viruses with and without associated organ lesions.

Of particular interest is the fact that serpentoviruses also infect nonepithelial cells distributed over the entire body, and specifically endothelial cells, intravascular monocytes, and extravascular macrophages within inflammatory processes, shown by our immunohistological approach. Our findings suggest that monocytes facilitate the systemic spread of the virus. Monocyte/macrophage infection is known to be a key process in the pathogenesis of other members of the order *Nidovirales*, such as feline coronaviruses (FCoV) (30), ferret systemic coronavirus (FRSCV) (31), and SARS-CoV (32). For FCoV, the ability to infect, replicate in, and activate monocytes and macrophages is essential in the pathogenesis of feline infectious peritonitis (FIP), a fatal disease of

felids. While the low-virulence feline enteric coronavirus (FECV) biotype primarily replicates in enterocytes and does only induce mild enteric disease, the highly virulent feline infectious peritonitis virus (FIPV) biotype predominantly arises after S gene mutations in FECV of the infected host that allow efficient replication in and systemic spread with monocytes (33). This allows rapid dissemination of the virus throughout the body (monocyte-associated viremia) and is a prerequisite of the monocyte activation with subsequent development of the granulomatous phlebitis that is the hallmark of FIP (30, 34, 35). A similar mechanism is likely for ferrets with a comparable disease and for experimental infections of interferon gamma (IFN- γ) knockout mice with mouse hepatitis virus (MHV) (31, 36). Similar to cats with FIP, systemically serpentovirus-infected pythons exhibited a multifocal macrophage-dominated vasculitis which was in severe cases associated with fibrinoid necrosis of the vessel wall but also appeared as chronic perivascular (pyo)granulomatous cuffs with abundant serpentovirus-positive macrophages. These vascular lesions could result from an interaction between activated serpentovirus-infected monocytes and endothelial cells, in particular, since the latter were also found to become infected. They might also be responsible for the broad spectrum of granulomatous to fibrinonecrotic lesions in organs, since these might at least partly be of ischemic nature.

Sequencing of the serpentovirus genomes did not reveal variants that would be associated with the systemic infection observed in some individuals. However, only experimental infections can provide hard evidence. The genome length and relatively high mutation and recombination rate of serpentoviruses makes identification of mutations that might alter the pathogenesis of the virus rather challenging. The S protein is the precursor of the spike complex that mediates receptor binding and entry, and thus, mutations in the S protein could most easily explain the differences in tissue tropism (37). However, we did not identify S protein mutations that would explain the different phenotypes. One could thus speculate that the different infection outcome is a consequence of differences in the host immune response.

During viral infections of mammals, viruses are recognized by pattern recognition receptors (PRRs) which induce a type I interferon (IFN) response, mediated by IFN- α and - β . The IFN response is considered the primary host defense mechanism against viral infections. It is therefore not surprising that many viruses have developed mechanisms to subvert or alter the type I IFN response (36). Interference of nidoviruses with the IFN response has so far mainly been investigated in the family *Coronaviridae*. In studies on human infection, the presence of viral proteins in monocytes was not found to be associated with significant IFN- α production, and it was suggested that viral particles had been taken up by monocytes via phagocytosis (38). This correlates with studies on IFN receptor-deficient knockout mice, where MHV infection was associated with higher viral titers and a broader tissue tropism of the virus (36). Further studies are needed to determine whether systemic serpentoviral infection in snakes is also related to an altered IFN response.

MATERIALS AND METHODS

Animals. The study included 30 pythons of 7 different species (green tree python, *Morelia viridis*; woma python, *Aspidites ramsayi*; carpet python, *Morelia spilota*; Angolan python, *Python anchietae*; ball python, *Python regius*; Indian python, *Python molurus*; black-headed python, *Aspidites melanocephalus*) with serpentovirus-associated disease, confirmed by immunohistology for serpentovirus nucleoprotein (NP) and reverse transcription-PCR (RT-PCR) (6) (Table 1). The animals had been submitted for a diagnostic postmortem examination upon the owners' request, either at the Institute of Veterinary Pathology, Vetsuisse Faculty, University of Zurich, or at the Pathology Unit, Universitat Autònoma de Barcelona, Spain, between 2012 and 2018. Most animals had died or been euthanized prior to submission; four individuals (CH-A4, CH-B1, CH-B2, E-B2) were submitted by the owner for euthanasia and immediate diagnostic examination. Euthanasia followed an ASPA (Animals Scientific Procedures Act 1986) schedule 1 (appropriate methods of humane killing [<http://www.legislation.gov.uk/ukpga/1986/14/schedule/1>]) procedure. A separate research permit was not required for the diagnosis-motivated necropsies and subsequent sample collection.

Most animals had presented clinically with respiratory signs, ranging from mild mucus secretion from the oral and nasal cavity to severe acute, recurrent, or chronic dyspnea. In some cases, the breeders reported repeated treatment attempts, occasionally for more than 1 year, prior to the animals' death,

which included frequent nebulizing with an antiseptic solution (F10 antiseptic solution-benzalkonium chloride and polyhexamethylene biguanide, Health and Hygiene [Pty] Ltd.) and/or antibiotic treatment with commercial broad-spectrum antibiotics such as enrofloxacin. In other cases, the animals had died suddenly without prior clinical signs (Table 1).

The affected snakes had a broad age range (3 months to 10 years; average, 3.65 years). Nineteen were male and ten were female; the sex of one young individual was unknown (undifferentiated genital organs). The animals originated from nine collections/breeding colonies of varying size (from a single snake up to a collection of 50 breeding animals) in Switzerland and Spain (Table 1). For most animals, information on their exact origin was not available anymore. Breeders CH-A, -B, -C, and -F, whose collection sizes ranged from approximately 40 to 50 individuals, had been exchanging/trading animals either between each other or with other breeders. Breeder CH-F stated that he had obtained the deceased individuals from a commercial trader. His animals are single-housed in terraria in two rooms (each approximately 25 m² in size) and kept at a "summer" room temperature of 27 to 30°C during the day and 25 to 28°C during the night and a "winter" temperature of 25 to 28°C during the day and 22 to 25°C during the night, at 50% to 90% humidity. For some specific species (*Morelia viridis*, *M. spilota*), terraria are sprayed with warm water 2 to 3 times per week. Breeder CH-A, on the other hand, reported that he keeps the snakes at a steady temperature of 23 to 25°C throughout the whole year and sprays the terraria with warm water only once per week. Hygiene measures taken by both breeders include disinfection of hands and tools (forceps etc.) with commonly used disinfectant solutions (F10 antiseptic solution-benzalkonium chloride and polyhexamethylene biguanide, Health and Hygiene [Pty] Ltd.) after handling each individual.

Sample collection and screening for infectious agents. All animals were subjected to a full postmortem examination, and samples from brain, lung, liver, and kidney were collected and stored at -80°C for further analysis. In addition, samples from all major organs and tissues (brain, respiratory tract, liver, kidney, spleen, gastrointestinal tract, reproductive tract, pancreas) were collected and fixed in 4% buffered formalin for histological and immunohistological examinations.

The lungs of some snakes were submitted to routine bacteriological examination, and from one animal, a virological examination for common respiratory snake viruses was undertaken (Table 1).

Histology, immunohistology, and immunofluorescence. Formalin-fixed tissue samples were trimmed and routinely paraffin wax embedded. Consecutive sections (4 to 5 μm) were prepared and stained with hematoxylin and eosin (HE) or subjected to immunohistological and immunofluorescence staining.

Sections from all histologically examined organs were subjected to immunohistological staining for serpentovirus NP, using a custom-made rabbit polyclonal antibody (anti-MVNV NP) and a previously described protocol (6). A formalin-fixed, paraffin-embedded cell pellet prepared from serpentovirus-infected cell cultures served as a positive control. Consecutive sections incubated with the preimmune serum instead of the specific primary antibody served as negative controls.

Sections from one individual (CH-A7) underwent immunofluorescence staining. After deparaffinization, they were incubated with anti-MVNV NP antibody at a 1:500 dilution (in phosphate-buffered saline [PBS]) overnight at 4°C, washed five times with PBS, incubated for 30 min at room temperature with a 1:500 dilution (in PBS) of Alexa Fluor 594-labeled goat anti-rabbit immunoglobulin secondary antibody (Invitrogen), and then washed four times with PBS. Afterward, the sections were incubated with an anti-Iba-1 antibody (ab5076; Biotec) at a 1:400 dilution (in PBS) overnight at 4°C, washed five times with PBS, and incubated for 30 min at room temperature with Alexa Fluor 488-labeled donkey anti-goat immunoglobulin secondary antibody (Invitrogen; 1:500 in PBS), followed by a 15-min incubation with DAPI (4',6'-diamidino-2-phenylindole; Novus Biologicals; 1:10,000 in PBS). Sections were washed twice with distilled water and air dried, and a coverslip was placed with FluoreGuard mounting medium (Biosystems, Switzerland). Images were taken at a ×400 magnification with a Nikon Eclipse Ni-U microscope with NIS Advanced Research software.

Virus isolation. Cultured brain and liver cells of *M. viridis*, at passages 8 to 15, were used for inoculations with tissue samples from selected animals (Table 1) as previously described (6). At 4 to 5 days postinoculation, the cell culture supernatants were collected for RT-PCR and next-generation sequencing (NGS) library preparation.

RT-PCR and NGS. RNA was extracted from lung and/or liver tissue samples of 24 animals, from cotton dry swabs used to sample the choanal and cloacal mucosa of 10 animals, from a lung lavage sample of an adult female ball python (*Python regius*) from another Swiss breeder unrelated to any of the others, and from tissue culture supernatants (Table 1) as previously described (6). Library preparation, data analysis, and genome assembly were done as previously described (6).

To study the frequencies of single nucleotide polymorphisms (SNPs) within samples, the NGS reads were quality filtered using Trimmomatic, and the reads with a Q-score over 30 were assembled against the consensus sequence of a given sample using the Burrows-Wheeler Aligner MEM (BWA-MEM) algorithm (39) followed by removal of potential PCR duplicates using SAMTools version 1.8 (40). The frequency of single nucleotide variants in each sequence position was called using LoFreq version 2 (41), and the genetic diversity between viral sequences derived from tissue and cell culture was compared using SNPGenie software (42).

Phylogenetic analysis. The reference sequences used in the phylogenetic analysis are listed in Table 2. The complete genomes of python-associated virus strains were aligned using the ClustalW algorithm implemented in the MEGA7 program (43). In addition, the amino acid sequences of ORF1b (RdRp) were aligned with MAFFT version 7.407 using E-INS-i parameters (44). The phylogenetic trees were constructed using the Bayesian Markov chain Monte Carlo (MCMC) method, implemented in MrBayes version 3.2 (45)

TABLE 2 List of reference sequences used in the sequence analysis

GenBank accession no.	Virus
GU002364	Fathead minnow nidovirus
KJ541759	Ball python nidovirus strain 07-53
KJ935003	Python nidovirus isolate S1536-13
KX184715	Shingleback nidovirus 1
KX883637.1	Xinzhou nematode virus 6
LC088094	Bovine torovirus
MF351889	Morelia viridis nidovirus strain S14-1323
MG996765	Equine torovirus
MN161560	Serpentovirinae sp. isolate A95
MN161563	Serpentovirinae sp. isolate F17
MN161564	Serpentovirinae sp. isolate H0-1
MN161565	Serpentovirinae sp. isolate H0-2
MN161567	Serpentovirinae sp. isolate L1
MN161568	Serpentovirinae sp. isolate L3
MN161569	Serpentovirinae sp. isolate L4
MK182566	Morelia viridis nidovirus isolate BH128 14-12
MK182569	Morelia viridis nidovirus isolate BH171 14-7
NC_007447	Breda virus Canada-1997
NC_008516	White bream virus
NC_022787	Porcine torovirus
NC_026812	Chinook salmon bafinivirus
NC_027199	Bovine nidovirus
NC_033700	Xinzhou toro-like virus

with two independent runs and four chains per run, the GTR-G-I model of substitution for nucleotides, and the WAG model of substitution for amino acids. The analyses were run for 5 million states and sampled every 5,000 steps.

Recombination analysis. Recombination events were sought from an alignment containing snake-associated serpentoviruses using the pairwise homoplasy index (PHI) test (46) implemented in SplitsTree version 4.15.1 (47) and the tree order scan method implemented in SSE 1.3 software (48), followed by identification of potentially recombinant sequences and estimation of recombination breakpoints using the RDP (49), bootscan (50), maxchi (51), chimera (52), 3seq (53), geneconv (54), and siscan (55) methods implemented in RDP4 software (56). The potential recombination events detected by at least five out of seven methods were further evaluated by constructing phylogenetic trees using the neighbor joining method and maximum composite likelihood substitution model implemented in MEGA7 software (43).

ACKNOWLEDGMENTS

We are grateful to the technical staff of the Histology Laboratory for excellent technical assistance.

The study was supported by the Academy of Finland (1308613) and the Finnish Foundation of Veterinary Research.

We also thank the snake owners for submitting the cases.

REFERENCES

- Beards GM, Campbell AD, Cottrell NR, Peiris JS, Rees N, Sanders RC, Shirley JA, Wood HC, Flewett TH. 1984. Enzyme-linked immunosorbent assays based on polyclonal and monoclonal antibodies for rotavirus detection. *J Clin Microbiol* 19:248–254. <https://doi.org/10.1128/JCM.19.2.248-254.1984>.
- Chandra AM, Jacobson ER, Munn RJ. 2001. Retroviral particles in neoplasms of Burmese pythons (*Python molurus bivittatus*). *Vet Pathol* 38:561–564. <https://doi.org/10.1354/vp.38-5-561>.
- Draker R, Roper RL, Petric M, Tellier R. 2006. The complete sequence of the bovine torovirus genome. *Virus Res* 115:56–68. <https://doi.org/10.1016/j.virusres.2005.07.005>.
- Sun H, Lan D, Lu L, Chen M, Wang C, Hua X. 2014. Molecular characterization and phylogenetic analysis of the genome of porcine torovirus. *Arch Virol* 159:773–778. <https://doi.org/10.1007/s00705-013-1861-x>.
- Bodewes R, Lempp C, Schurch AC, Habierski A, Hahn K, Lamers M, von Dornberg K, Wohlsein P, Drexler JF, Haagmans BL, Smits SL, Baumgartner W, Osterhaus ADME. 2014. Novel divergent nidovirus in a python with pneumonia. *J Gen Virol* 95:2480–2485. <https://doi.org/10.1099/vir.0.068700-0>.
- Dervas E, Hepojoki J, Laimbacher A, Romero-Palomo F, Jelinek C, Keller S, Smura T, Hepojoki S, Kipar A, Hetzel U. 2017. Nidovirus-associated proliferative pneumonia in the green tree python (*Morelia viridis*). *J Virol* 91:e00718-17. <https://doi.org/10.1128/JVI.00718-17>.
- Hoon-Hanks LL, Layton ML, Ossiboff RJ, Parker JSL, Dubovi EJ, Stenglein MD. 2018. Respiratory disease in ball pythons (*Python regius*) experimentally infected with ball python nidovirus. *Virology* 517:77–87. <https://doi.org/10.1016/j.virol.2017.12.008>.
- Marschang RE, Kolesnik E. 2017. Detection of nidoviruses in live pythons and boas. *Tierarztl Prax Ausg K Kleintiere Heimtiere* 45:22–26. <https://doi.org/10.15654/TPK-151067>.
- O'Dea MA, Jackson B, Jackson C, Xavier P, Warren K. 2016. Discovery and partial genomic characterisation of a novel nidovirus associated with respiratory disease in wild shingleback lizards (*Tiliqua rugosa*). *PLoS One* 11:e0165209. <https://doi.org/10.1371/journal.pone.0165209>.
- Stenglein MD, Jacobson ER, Wozniak EJ, Wellehan JFX, Kincaid A, Gordon M, Porter BF, Baumgartner W, Stahl S, Kelley K, Towner JS, DeRisi JL. 2014. Ball python nidovirus: a candidate etiologic agent for severe respiratory disease in *Python regius*. *mBio* 5:e01484-14–e01414. <https://doi.org/10.1128/mBio.01484-14>.

11. Uccellini L, Ossiboff RJ, de Matos REC, Morrisey JK, Petrosov A, Navarrete-Macias I, Jain K, Hicks AL, Buckles EL, Tokarz R, McAloose D, Lipkin WI. 2014. Identification of a novel nidovirus in an outbreak of fatal respiratory disease in ball pythons (*Python regius*). *Virology* 11:144. <https://doi.org/10.1186/1743-422X-11-144>.
12. Zhang J, Finlaison DS, Frost MJ, Gestier S, Gu X, Hall J, Jenkins C, Parrish K, Read AJ, Srivastava M, Rose K, Kirkland PD. 2018. Identification of a novel nidovirus as a potential cause of large scale mortalities in the endangered Bellinger River snapping turtle (*Myuchelys georgesii*). *PLoS One* 13:e0205209. <https://doi.org/10.1371/journal.pone.0205209>.
13. Cundall D, Tuttmann C, Close M. 2014. A model of the anterior esophagus in snakes, with functional and developmental implications. *Anat Rec (Hoboken)* 297:586–598. <https://doi.org/10.1002/ar.22860>.
14. Hoon-Hanks LL, Ossiboff RJ, Bartolini P, Fogelson SB, Perry SM, Stöhr AC, Cross ST, Wellehan JFX, Jacobson ER, Dubovi EJ, Stenglein MD. 2019. Longitudinal and cross-sectional sampling of serpentovirus (Nidovirus) infection in captive snakes reveals high prevalence, persistent infection, and increased mortality in pythons and divergent serpentovirus infection in boas and colubrids. *Front Vet Sci* 6:338. <https://doi.org/10.3389/fvets.2019.00338>.
15. Blahak S, Jenckel M, Höper D, Beer M, Hoffmann B, Schlottau K. 2020. Investigations into the presence of nidoviruses in pythons. *Virology* 17:6. <https://doi.org/10.1186/s12985-020-1279-5>.
16. Starck JM, Weimer I, Aupperle H, Müller K, Marschang RE, Kiefer I, Pees M. 2015. Morphological pulmonary diffusion capacity for oxygen of burmese pythons (*Python molurus*). A comparison of animals in healthy condition and with different pulmonary infections. *J Comp Pathol* 153:333–351. <https://doi.org/10.1016/j.jcpa.2015.07.004>.
17. Imai M, Shibata T, Moriguchi K. 1991. Pepsinogen granules in the esophageal epithelium of the rock snake. *Okajimas Folia Anat Jpn* 68:231–234.
18. Hu Z-M, Yang Y-L, Xu L-D, Wang B, Qin P, Huang Y-W. 2019. Porcine torovirus (PToV): a brief review of etiology, diagnostic assays and current epidemiology. *Front Vet Sci* 6:120. <https://doi.org/10.3389/fvets.2019.00120>.
19. Koopmans M, van den Boom U, Woode G, Horzinek MC. 1989. Seroepidemiology of Breda virus in cattle using ELISA. *Vet Microbiol* 19:233–243. [https://doi.org/10.1016/0378-1135\(89\)90069-2](https://doi.org/10.1016/0378-1135(89)90069-2).
20. Brown DW, Selvakumar R, Daniel DJ, Mathan VI. 1988. Prevalence of neutralising antibodies to Berne virus in animals and humans in Vellore, South India. Brief report. *Arch Virol* 98:267–269. <https://doi.org/10.1007/BF01322174>.
21. Dhama K, Pawaiya RVS, Chakraborty S, Tiwari R, Verma AK. 2014. Toroviruses affecting animals and humans. A review. *Asian J Animal and Veterinary Advances* 9:190–201. <https://doi.org/10.3923/ajava.2014.190.201>.
22. Hoet AE, Cho K-O, Chang K-O, Loerch SC, Wittum TE, Saif LJ. 2002. Enteric and nasal shedding of bovine torovirus (Breda virus) in feedlot cattle. *Am J Vet Res* 63:342–348. <https://doi.org/10.2460/ajvr.2002.63.342>.
23. Mackay IM, Arden KE. 2015. MERS coronavirus: diagnostics, epidemiology and transmission. *Virology* 12:222. <https://doi.org/10.1186/s12985-015-0439-5>.
24. Pan Y, Zhang D, Yang P, Poon LLM, Wang Q. 2020. Viral load of SARS-CoV-2 in clinical samples. *Lancet Infect Dis* 20:411–412. [https://doi.org/10.1016/S1473-3099\(20\)30113-4](https://doi.org/10.1016/S1473-3099(20)30113-4).
25. Jamieson FB, Wang EE, Bain C, Good J, Duckmanton L, Petric M. 1998. Human torovirus. A new nosocomial gastrointestinal pathogen. *J Infect Dis* 178:1263–1269. <https://doi.org/10.1086/314434>.
26. Koopmans M, Horzinek MC. 1995. The pathogenesis of torovirus infections in animals and humans, p 403–413. In Siddell SG (ed), *The Coronaviridae*. Springer, Boston, MA.
27. Reynolds DJ. 1983. Coronavirus replication in the intestinal and respiratory tracts during infection of calves. *Ann Rech Vet* 14:445–446.
28. Yang XY, Yao GH, Xu J, Zhong NS. 2006. The possible mechanism of lung injury induced by severe acute respiratory syndrome coronavirus spike glycoprotein. *Zhonghua Jie He He Hu Xi Za Zhi* 29:587–590. (In Chinese.)
29. Guo Y-R, Cao Q-D, Hong Z-S, Tan Y-Y, Chen S-D, Jin H-J, Tan K-S, Wang D-Y, Yan Y. 2020. The origin, transmission and clinical therapies on coronavirus disease 2019 (COVID-19) outbreak: an update on the status. *Mil Med Res* 7:11. <https://doi.org/10.1186/s40779-020-00240-0>.
30. Kipar A, May H, Menger S, Weber M, Leukert W, Reinacher M. 2005. Morphologic features and development of granulomatous vasculitis in feline infectious peritonitis. *Vet Pathol* 42:321–330. <https://doi.org/10.1354/vp.42-3-321>.
31. Doria-Torra G, Vidaña B, Ramis A, Amarilla SP, Martínez J. 2016. Coronavirus infection in ferrets: antigen distribution and inflammatory response. *Vet Pathol* 53:1180–1186. <https://doi.org/10.1177/0300985816634809>.
32. Cheung CY, Poon LLM, Ng IHY, Luk W, Sia S-F, Wu MHS, Chan K-H, Yuen K-Y, Gordon S, Guan Y, Peiris J. 2005. Cytokine responses in severe acute respiratory syndrome coronavirus-infected macrophages in vitro: possible relevance to pathogenesis. *J Virol* 79:7819–7826. <https://doi.org/10.1128/JVI.79.12.7819-7826.2005>.
33. Malbon AJ, Meli ML, Barker EN, Davidson AD, Tasker S, Kipar A. 2019. Inflammatory mediators in the mesenteric lymph nodes, site of a possible intermediate phase in the immune response to feline coronavirus and the pathogenesis of feline infectious peritonitis? *J Comp Pathol* 166:69–86. <https://doi.org/10.1016/j.jcpa.2018.11.001>.
34. Kipar A, Meli ML. 2014. Feline infectious peritonitis. Still an enigma? *Vet Pathol* 51:505–526. <https://doi.org/10.1177/0300985814522077>.
35. Rottier PJM, Nakamura K, Schellen P, Volders H, Haijema BJ. 2005. Acquisition of macrophage tropism during the pathogenesis of feline infectious peritonitis is determined by mutations in the feline coronavirus spike protein. *J Virol* 79:14122–14130. <https://doi.org/10.1128/JVI.79.22.14122-14130.2005>.
36. Roth-Cross JK, Bender SJ, Weiss SR. 2008. Murine coronavirus mouse hepatitis virus is recognized by MDA5 and induces type I interferon in brain macrophages/microglia. *J Virol* 82:9829–9838. <https://doi.org/10.1128/JVI.01199-08>.
37. Jaimes JA, Whittaker GR. 2018. Feline coronavirus: insights into viral pathogenesis based on the spike protein structure and function. *Virology* 517:108–121. <https://doi.org/10.1016/j.virol.2017.12.027>.
38. Yilla M, Harcourt BH, Hickman CJ, McGrew M, Tamin A, Goldsmith CS, Bellini WJ, Anderson LJ. 2005. SARS-coronavirus replication in human peripheral monocytes/macrophages. *Virus Res* 107:93–101. <https://doi.org/10.1016/j.virusres.2004.09.004>.
39. Li H. 2013. Aligning sequence reads, clone sequences and assembly contigs with BWA-MEM. *arXiv* 1303.3997. <https://arxiv.org/abs/1303.3997>.
40. Li H. 2011. A statistical framework for SNP calling, mutation discovery, association mapping and population genetical parameter estimation from sequencing data. *Bioinformatics* 27:2987–2993. <https://doi.org/10.1093/bioinformatics/btr509>.
41. Wilm A, Aw PPK, Bertrand D, Yeo GHT, Ong SH, Wong CH, Khor CC, Petric R, Hibberd ML, Nagarajan N. 2012. LoFreq: a sequence-quality aware, ultra-sensitive variant caller for uncovering cell-population heterogeneity from high-throughput sequencing datasets. *Nucleic Acids Res* 40:11189–11201. <https://doi.org/10.1093/nar/gks918>.
42. Nelson CW, Moncla LH, Hughes AL. 2015. SNPGenie: estimating evolutionary parameters to detect natural selection using pooled next-generation sequencing data. *Bioinformatics* 31:3709–3711. <https://doi.org/10.1093/bioinformatics/btv449>.
43. Kumar S, Stecher G, Tamura K. 2016. MEGA7. Molecular Evolutionary Genetics Analysis Version 7.0 for bigger datasets. *Mol Biol Evol* 33:1870–1874. <https://doi.org/10.1093/molbev/msw054>.
44. Katoh K, Standley DM. 2013. MAFFT multiple sequence alignment software version 7. Improvements in performance and usability. *Mol Biol Evol* 30:772–780. <https://doi.org/10.1093/molbev/mst010>.
45. Ronquist F, Teslenko M, van der Mark P, Ayres DL, Darling A, Höhna S, Larget B, Liu L, Suchard MA, Huelsenbeck JP. 2012. MrBayes 3.2. Efficient Bayesian phylogenetic inference and model choice across a large model space. *Syst Biol* 61:539–542. <https://doi.org/10.1093/sysbio/sys029>.
46. Bruen TC, Philippe H, Bryant D. 2006. A simple and robust statistical test for detecting the presence of recombination. *Genetics* 172:2665–2681. <https://doi.org/10.1534/genetics.105.048975>.
47. Huson DH, Bryant D. 2006. Application of phylogenetic networks in evolutionary studies. *Mol Biol Evol* 23:254–267. <https://doi.org/10.1093/molbev/msj030>.
48. Simmonds P. 2012. SSE: a nucleotide and amino acid sequence analysis platform. *BMC Res Notes* 5:50. <https://doi.org/10.1186/1756-0500-5-50>.
49. Martin D, Rybicki E. 2000. RDP: detection of recombination amongst aligned sequences. *Bioinformatics* 16:562–563. <https://doi.org/10.1093/bioinformatics/16.6.562>.
50. Salminen MO, Carr JK, Burke DS, McCutchan FE. 1995. Identification of breakpoints in intergenotypic recombinants of HIV type 1 by bootscanning. *AIDS Res Hum Retroviruses* 11:1423–1425. <https://doi.org/10.1089/aid.1995.11.1423>.

51. Smith JM. 1992. Analyzing the mosaic structure of genes. *J Mol Evol* 34:126–129. <https://doi.org/10.1007/BF00182389>.
52. Posada D, Crandall KA. 2001. Evaluation of methods for detecting recombination from DNA sequences: computer simulations. *Proc Natl Acad Sci U S A* 98:13757–13762. <https://doi.org/10.1073/pnas.241370698>.
53. Boni MF, Posada D, Feldman MW. 2007. An exact nonparametric method for inferring mosaic structure in sequence triplets. *Genetics* 176:1035–1047. <https://doi.org/10.1534/genetics.106.068874>.
54. Padidam M, Sawyer S, Fauquet CM. 1999. Possible emergence of new geminiviruses by frequent recombination. *Virology* 265:218–225. <https://doi.org/10.1006/viro.1999.0056>.
55. Gibbs MJ, Armstrong JS, Gibbs AJ. 2000. Sister-Scanning: a Monte Carlo procedure for assessing signals in recombinant sequences. *Bioinformatics* 16:573–582. <https://doi.org/10.1093/bioinformatics/16.7.573>.
56. Martin DP, Murrell B, Golden M, Khoosal A, Muhire B. 2015. RDP4: detection and analysis of recombination patterns in virus genomes. *Virus Evol* 1:vev003.